PHYSICAL REVIEW B **82**, 121301(R) (2010)

Experimental test for geminate recombination applied to organic solar cells

R. A. Street*
Palo Alto Research Center, Palo Alto, California 94304, USA

Sarah Cowan and A. J. Heeger
Center for Polymers and Organic Solids, University of California at Santa Barbara, Santa Barbara, California 93106, USA

(Received 18 August 2010; published 1 September 2010)

We show that a clear experimental test can distinguish between geminate and nongeminate recombination in low mobility semiconductors. For the particular case of the organic solar cell, the relative contribution of geminate recombination can be determined by measuring transient photoconductivity versus applied voltage. Measurements carried out at room temperature and 200 K on bulk heterojunction organic solar cells fabricated with two different semiconducting polymers show that neither exhibits significant geminate recombination.

DOI: 10.1103/PhysRevB.82.121301 PACS number(s): 73.50.Gr, 88.40.jr, 72.20.Jv, 72.80.Le

Geminate recombination occurs in a semiconductor when the recombining electron and hole were both created by the same absorbed photon. This mechanism is specific to low mobility, low conductivity, and, typically, disordered semiconductors; in a crystalline material, the delocalized electron and hole quickly lose their spatial correlation. Geminate recombination is implicated in amorphous selenium,[1] amorphous silicon at low temperature,[2] polymer and small molecule photoconductors,[3,4] and recently in organic bulk heterojunction (BHJ) solar cells. This Rapid Communication shows that geminate and nongeminate recombination mechanisms lead to distinctly different testable predictions. Measurements of transient photoconductivity versus applied voltage on operating solar cells provide the required information. We apply the technique to two types of BHJ solar cells and find that geminate recombination is not significant in either.

The defining difference in the recombination mechanisms is that geminate recombination occurs before mobile "free" carriers are created and nongeminate recombination occurs afterward. Even when there is significant diffusion of the electron and hole before geminate recombination, the fact that the recombining electron and hole are the same pair that was created, means that neither contributes to the net current flow. This conclusion is true even when the recombination occurs at a different location from the absorption; any contribution to an external current by the motion of one carrier is cancelled by the offsetting motion of the carrier of the other sign.

The displacement charge is qx/d, when a charge q, moves a distance x in a parallel-plate photoconductor of thickness d, and the oppositely charged member of the geminate pair has displacement charge $-qx/d$. If the charges are created at position x_1 and recombine at x_2, there is net zero induced charge for the pair. Although one particular pair induces a small time-varying current,

$$\frac{q}{d}\frac{d}{dt}[x_h(t) - x_e(t)]$$

as a result of the independent diffusive motion of the electron (e) and hole (h), the time-integrated contribution to the current from the pair is zero, because they are created and recombine together. Moreover, the ensemble of uncorrelated pairs ensures that the instantaneous current also averages to zero. In contrast, when recombination is nongeminate, electrons and holes are separated, and the displacement current before any recombination is

$$I_D = q_e\mu_e E/d + q_h\mu_h E/d, \tag{1}$$

where μ_e, μ_h are the electron and hole mobility, E is the electric field and d is the film thickness. The two terms in Eq. (1) add rather than cancel because the electron and hole move in opposite directions in response to the internal electric field.

Measurement of the initial mobile carrier density as the recombination probability changes therefore distinguishes geminate and nongeminate recombination, as we show in more detail for the specific case of the BHJ organic solar cell. In these cells, ultrafast photoinduced electron transfer across the buried donor-acceptor interface creates holes in the donor and electrons in the acceptor domains, both of which are transported to the electrodes by the internal electric field.[5,6] Even in the best cells, recombination causes a reduction in the fill factor and a loss of cell efficiency. The cell current $I_P(V)$, can be described by[7]

$$I_P(V) = I_D(V) - eP_R(V)G, \tag{2}$$

where $I_D(V)$ is the dark current at voltage V. $P_R(V)$ is the normalized photocurrent and reflects the bias-dependent collection of carriers, while G is the effective generation rate, excluding any loss of optical excitations that do not reach the donor-acceptor interface.

There has been much discussion of the recombination processes that determine $P_R(V)$. Geminate recombination of the charge-transfer exciton (CTE), formed from the separated electron-hole pair, has been considered an important mechanism in BHJ materials.[8–10] Previous studies have interpreted the cell characteristics on the basis of electric field ionization of the geminate CTE,[11–13] usually based on the Braun-Onsager model.[14,15] However nongeminate bimolecular recombination of electrons and holes by the Langevin mechanism[16,17] or Shockley-Read-Hall (SRH) recombination at interface states,[7,18] have also been proposed.

Geminate recombination attributes the voltage dependence of $P_R(V)$ to electric field ionization of the CTE, which generates mobile carriers at high bias and suppresses their formation at low bias. The mobile charge is assumed to be collected at the electrodes with high probability. In contrast, when nongeminate recombination is the dominant mechanism, the initial mobile charge density is independent of voltage, and mobile charge is lost by recombination during transport to the device contacts.

In either case $P_R(V)$ describes the competition between recombination and charge collection at the electrodes. $P_R(V)$ tends to unity in reverse bias and goes to zero when the applied voltage equals the diode built-in potential, V_{BI} and the internal electric field, E_{INT}, is zero. V_{BI} is usually in the range 0.5–1 V and is typically slightly larger than the cell open circuit voltage at 1 sun intensity

The test for geminate recombination is performed by measurements of the transient photoconductivity vs applied voltage in operating solar cells. Consider the charge created by a short illumination pulse. The collected charge, $Q(V_I)$, at an internal voltage, V_I, is the product of the initial mobile charge density, $N_0(V_I)$, and the probability of collection $F_C(V_I)$, $Q(V_I)=eN_0(V_I)F_C(V_I)$, and for the two recombination mechanisms,

$$\text{Geminate;}\quad Q(V_I) = eN_0(V_I)F_C,\quad \text{with}\quad F_C \sim 1, \tag{3}$$

$$\text{Nongeminate;}\quad Q(V_I) = eN_0F_C(V_I),\quad \text{with}\quad N_0 \sim \text{constant}. \tag{4}$$

Hence, measurement of $N_0(V_I)$, compared to the total charge collection distinguishes the two models. Transient photoconductivity provides the information because it can measure the current from the mobile carriers at short times before either significant recombination or charge collection has occurred. $Q(V_I)$ is equivalent to $eP_R(V_I)G$ provided that transient photoconductivity measures the same process as that which occurs during steady-state illumination.

Transient photoconductivity measurements, $I_P(V,t)$, have been applied successfully to organic semiconductors and BJH materials to measure the carrier mobility and recombination.[19,20] The carrier transit time, τ_T, across a sample of thickness, d, yields the mobility, $\mu=d^2/V_I\tau_T$. When recombination or deep trapping of the carrier occurs before the transit, then instead the lifetime, τ_R, is measured. Generalizing Eq. (1), the initial carrier concentration at an applied voltage, V, is given by

$$I_P(V,0+) = e(\mu_e + \mu_h)\int_0^d n_0(x,V)E_I(x)dx, \tag{5}$$

where $t=0+$ denotes just after the illumination pulse, $n_0(x,V)$ is the spatial profile of the initial carrier distribution and $E_I(x)$ is the internal electric field profile. The mechanism of exciton splitting ensures that $n_0(x,V)$ is identical for both electrons and holes. When either $E_I(x)$ or $n_0(x,V)$ are reasonably independent of x, both of which are expected since the sample is thin, then,

$$\frac{I_P(V,0+)}{V_{BI}-V} = N_0(V)e(\mu_e+\mu_h)/d, \tag{6}$$

where $N_0(V)$ is the total initial charge density and V_{BI} is the diode built-in potential, so that $V_I=V_{BI}-V$. The total charge measured in the transient is

$$Q(V) = \int_0^\infty I_P(V,t)dt. \tag{7}$$

Hence, transient photoconductivity provides values for both $N_0(V)$ and $Q(V)$.

The experiments were performed on solar cells fabricated from P3HT/PCBM and PCDTBT/$PC_{(70)}BM$.[21] The cells are about 100 nm thick and their fabrication and properties are described elsewhere.[4,22] The excitation source is a nitrogen pumped dye laser emitting a pulse of <10 ns duration at ~ 520 nm, which is above the band gap of the polymers and the $PC_{(70)}BM$. The current is measured from the voltage drop across a small resistor ($R=4$, 10, or 50 Ω) in series with the cell and is recorded on a digital oscilloscope. Several conditions need to be fulfilled for an accurate measurement of the carrier dynamics. The excitation charge should be less than CV, where C is the device capacitance so that space-charge effects do not alter the internal field. Since the applied voltages are small, the voltage developed across the load must also be small compared to the internal voltage. The illumination intensity was adjusted accordingly so that the charge is $<20\%$ of CV and the peak voltage is <0.15 V in reverse bias decreasing to ~ 10 mV in forward bias. The RC time constant of the external circuit (including both series and parallel resistances) must be short compared to the response time, hence the small load resistor. However, because the capacitance is large, the RC time constant does influence the fastest measured transients. The measurements were made with a 1 Hz pulse rate to allow any trapped charge to disperse, and the current transient is an average of up to 64 measurements.

Figure 1 shows the transient photoconductivity plotted as $I_P(V,t)/(V_{BI}-V)$ for a P3HT/PCBM cell measured at room temperature and as a function of applied bias from -1 V reverse bias, to 0.6 V forward bias. In reverse bias the current transient is complete after ~ 3 μs while in forward bias the current is observable to at least 25 μs. The voltage-normalized peak photocurrent is reasonably constant for $V>0$ V. Figure 2 shows $N_0(V)$ derived from the peak data in Fig. 1. $Q(V)$ obtained from transient photoconductivity and $P_R(V)$ from the dc measurements are also shown and the data confirm that they are identical. V_{BI}(=0.72 V) is the voltage at which the charge drops to zero and is obtained directly from the measurements. Hence the voltage dependence of $N_0(V)$ involves only measured quantities and material constants.

The resulting $N_0(V)$ is approximately independent of bias for applied voltages from 0.2 to 0.6 V which is the voltage range where $P_R(V)$ decreases rapidly toward zero. The apparent decrease in $N_0(V)$ in reverse bias is due to the limitations of the RC time constants. The combination of small series and shunt resistances gives a finite rise and fall time

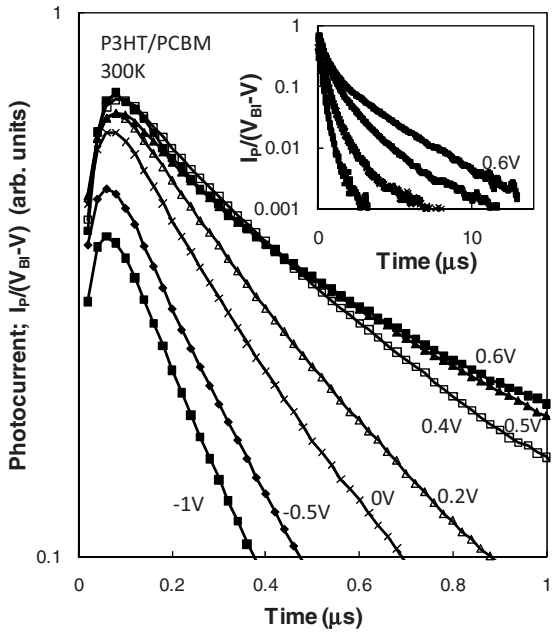

FIG. 1. Voltage-normalized transient photoconductivity, $I_P(V)/(V_{BI}-V)$, at different applied voltages as indicated, for a P3HT/PCBM solar cell at room temperature. The inset shows the same data over an extended time, for applied voltage, −1, 0, 0.4, and 0.6 V (left to right).

and a peak to the photocurrent transient at about 80 ns. At this time, a fraction $\mu tE/d$ of carriers have already reached the contact and no longer contribute to the photocurrent. For a mobility of 4×10^{-4} $\mathrm{cm}^2/\mathrm{V\ s}$, estimated from the transient response, we calculate that the loss of carriers is ~2% at 0.6 V but increases steadily to 40% at −1 V. Figure 2 shows the corrected values of $N_0(V)$, which are independent of bias voltage within experimental uncertainty.

Since the room-temperature drop in $P_R(V)$ occurs over

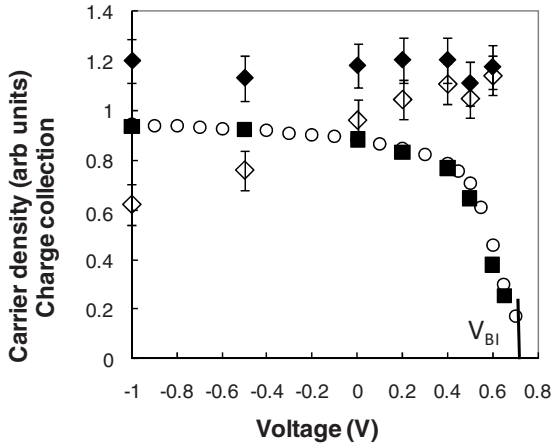

FIG. 2. The initial carrier densities, $N_0(V)$, in the P3HT/PCBM cell at room temperature, obtained from Eq. (6) for different bias voltages (open diamonds), and the same data corrected for the *RC* time constant of the electronics (closed diamonds). The figure also shows the normalized integrated charge, $Q(V)$ obtained from Eq. (7) (solid squares) and the dc current-voltage data, $P_R(V)$ (open circles). The extrapolated value of V_{BI} is indicated.

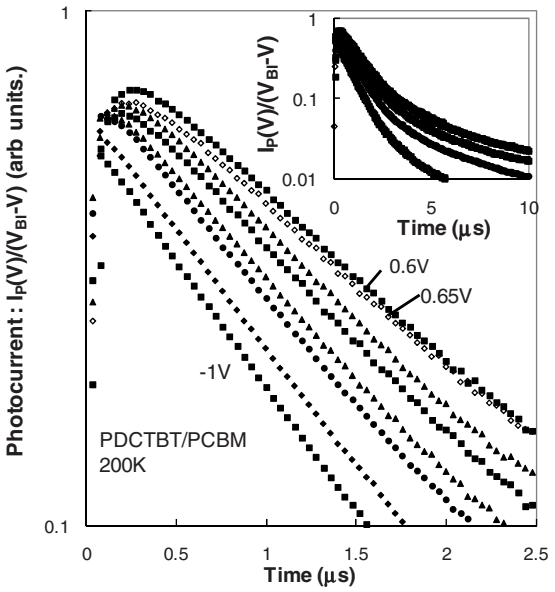

FIG. 3. Voltage-normalized transient photoconductivity, $I_P(V)/(V_{BI}-V)$, at different applied voltages (0.65, 0.6, 0.5, 0.4, 0.2, 0, −0.5, and −1 V) for a PCDTBT/$PC_{(70)}$BM solar cell, measured at 200 K. The inset shows the same data over an extended time, for applied voltage, −1, 0, 0.4, and 0.6 V (left to right).

only a limited voltage range, and there are temporal resolution limits because of the *RC* time constant effect, the experiment was repeated at low temperature, where the drop in $P_R(V)$ is more extended in voltage and the mobility is lower. Figure 3 shows the voltage-normalized transient photoconductivity data measured at 200 K, in a solar cell made from PCDTBT/$PC_{(70)}$BM. The room-temperature data for this device are similar in form to the results obtained from the P3HT device. Figure 4 shows $Q(V)$, the steady-state data, and the initial mobile charge density, obtained exactly as for the room-temperature data. The initial carrier concentration is again found to be constant within experimental uncertainty over a wider voltage range and as the charge collection drops to 20% of its saturation value.

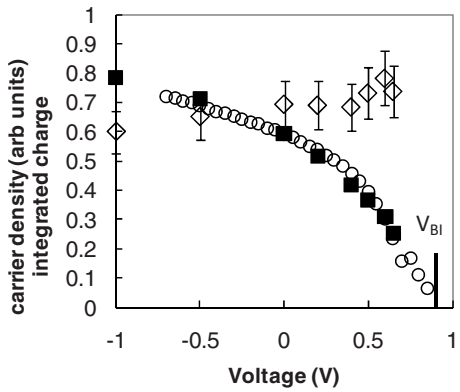

FIG. 4. The initial carrier densities, $N_0(V)$, in the PCDTBT/$PC_{(70)}$BM cell at 200 K, for different bias voltages (open diamonds). The figure also shows the normalized integrated charge, $Q(V)$ (solid squares) and the dc current-voltage data, $P_R(V)$ (open circles). The extrapolated value of V_{BI} is indicated.

The application of Eq. (6) to obtain the initial carrier concentration is based on assumptions that need further discussion. First, the model assumes a fixed electron and hole mobility. There is evidence that the mobility of the cell material is dispersive[18] with the typical power-law decrease with time. Dispersive mobility exhibits an effective dependence on electric field because the transit time, and hence the apparent mobility, change with field. However the dispersive mobility is constant in time and field when comparing data at a fixed time, as in these measurements of N_0. Second, equating the built-in potential with the voltage at which the dc photocurrent crosses zero is correct provided the series resistance of the cell is negligible. This requirement is confirmed from measurements of the dark forward bias cell current which does not show significant series resistance until $V > V_{BI}$ in either cell.

Figures 2 and 4 both show that the initial mobile charge density is independent of bias and, in particular, definitely does not decrease in proportion to $P_R(V)$. The results are consistent only with the expectations for nongeminate recombination and therefore imply that geminate recombination is not significant in these cells either at room temperature or at 200 K. Since geminate recombination is widely observed in bulk polymer semiconductors, it may seem surprising that it is not significant in these BHJ cells. The contribution of geminate recombination depends largely on the binding energy, E_B, of the exciton formed by the generated electron and hole.[14,23] While E_B is large in a many bulk organic semiconductors, the separation of the pair at the interface of the BHJ cell reduces the binding energy, increasing the probability that the electron and hole separate rather than recombine.

In summary we have shown that there is a clear experimental test for geminate recombination. Measurements performed on two BJH solar cells lead to the conclusion that recombination must occur from nongeminate loss of mobile carriers. Geminate CTE recombination should show an initial charge density that is proportional to the dc solar cell current and is clearly inconsistent with the measurements. The accuracy of the result is estimated to be $\sim 10-15\ \%$, which is therefore the upper bound on the contribution of geminate recombination; the main source of uncertainty arises from the effect of the RC time constant on the measured value of the initial photocurrent and from uncertainty in the value of V_{BI}. Since the relative importance of geminate or nongeminate recombination depends on the specific materials comprising the cell and possibly on the method of preparation, other cells may or may not have a larger geminate recombination contribution. Our results provide a technique to test the many different BHJ cells for geminate recombination.

Research at UCSB was supported as part of the Center for Energy Efficient Materials, an Energy Frontier Research Center funded by the U.S. Department of Energy, Office of Science, Office of Basic Energy Sciences under Award No. DE-SC0001009. A.J.H. and S.C. thank Anshuman Roy for many important comments and discussions. The materials used for the fabrication of the solar cells were provided by D. Waller of Konarka Technologies.

*street@parc.com

[1] J. C. Knights and E. A. Davis, J. Phys. Chem. Solids **35**, 543 (1974).
[2] C. Tsang and R. A. Street, Phys. Rev. B **19**, 3027 (1979); R. A. Street, *Hydrogenated Amorphous Silicon* (Cambridge University press, Cambridge, England, 1991), p. 300.
[3] D. M. Pai and R. C. Enck, Phys. Rev. B **11**, 5163 (1975).
[4] M. Pope and C. E. Swenberg, Annu. Rev. Phys. Chem. **35**, 613 (1984).
[5] G. Yu, J. Gao, J. C. Hummelen, F. Wudl, and A. J. Heeger, Science **270**, 1789 (1995).
[6] J. J. M. Halls, C. A. Walsh, N. C. Greenham, E. A. Marseglia, R. H. Friend, S. C. Moratti, and A. B. Holmes, Nature (London) **376**, 498 (1995).
[7] R. A. Street, M. Schoendorf, A. Roy, and J. H. Lee, Phys. Rev. B **81**, 205307 (2010).
[8] V. D. Mihailetchi, L. J. A. Koster, J. C. Hummelen, and P. W. M. Blom, Phys. Rev. Lett. **93**, 216601 (2004).
[9] D. Veldman, O. Ipek, S. C. J. Maskers, J. Sweelssen, M. M. Koetse, S. C. Veenstra, J. M. Kroon, S. S. van Bavel, J. Loos, and R. A. J. Janssen, J. Am. Chem. Soc. **130**, 7721 (2008).
[10] A. Liu, S. Zhao, S.-B. Rim, J. Wu, M. Könemann, P. Erk, and P. Peumans, Adv. Mater. **20**, 1065 (2008).
[11] K. Maturová, S. S. van Bavel, M. M. Wienk, R. A. J. Janssen, and M. Kemerink, Nano Lett. **9**, 3032 (2009).
[12] R. A. Marsh, C. R. McNeil, A. Abrusci, A. R. Campbell, and R. H. Friend, Nano Lett. **8**, 1393 (2008).
[13] J. Szmytkowski, Semicond. Sci. Technol. **25**, 015009 (2010).
[14] C. L. Braun, J. Chem. Phys. **80**, 4157 (1984).
[15] M. Wojcik and M. Tachiya, J. Chem. Phys. **130**, 104107 (2009).
[16] L. J. A. Koster, V. D. Mihailetchi, and P. W. M. Blom, Appl. Phys. Lett. **88**, 052104 (2006).
[17] G. Juska, K. Genevicius, G. Sliauzys, N. Nekrasas, and R. Osterbacka, J. Non-Cryst. Solids **354**, 2858 (2008).
[18] M. M. Mandoc, F. B. Kooistra, J. C. Hummerlen, B. de Boer,and P. W. M. Blom, Appl. Phys. Lett. **91**, 263505 (2007).
[19] C. R. McNeill and N. C. Greenham, Appl. Phys. Lett. **93**, 203310 (2008).
[20] C. G. Shuttle, B. O'Regan, A. M. Ballantyne, J. Nelson, D. D. C. Bradley, J. de Mello, and J. R. Durrant, Appl. Phys. Lett. **92**, 093311 (2008).
[21] PCDTBT is Poly[N-9′-hepta-decanyl-2,7-carbazole-alt-5,5-(4′,7′-di-2-thienyl-2′,1′,3′-benzothiadiazole); $PC_{(70)}BM$ is [6-6]-phenyl $C_{61(70)}$-butyric acid methyl ester; P3HT is poly(3-hexylthiophene).
[22] J. Y. Kim, S. H. Kim, H.-H. Lee, K. Lee, W. Ma, X. Gong, and A. J. Heeger, Adv. Mater. **18**, 572 (2006).
[23] R. A. Street, Appl. Phys. Lett. **93**, 133308 (2008).